Istraživanja i projektovanja za privredu
ISSN 1451-4117
DOI:10.5937/jaes0-42646
www.engineeringscience.rs

iipp publishing

Journal of Applied Engineering Science
Vol. 21, No. 2, 2023
Original Scientific Paper
Paper number: 21(2023)2, 1114, 729-740

INTERCEPTOR'S EFFECT ON TURNING MANEUVER PERFORMANCE WITH OPEN FREE RUNNING MODEL TEST METHOD

Muhammad Alimul Hafiz, Aries Sulisetyono*

Department of Naval Architecture, Institut Teknologi Sepuluh Nopember, Surabaya, Indonesia
** sulisea@na.its.ac.id*

It is necessary for the ship to have the capability of maneuvering when it is operating out at sea in order to protect the ship from the risk of colliding with other objects. To increase maneuverability, it is proposed to deploy interceptor devices on the two sides of the ship's stern, where the height of the interceptor blades can be adjusted. The working principle is to restrict the flow of fluid on one side at the stern in order to generate greater pressure than the other side, so that the fluid flowing towards the stern of the ship experiences a high-speed difference between one side and the other, resulting in an increase in side force. In this paper, the open free-running test method is used to test the interceptor's ability to turn on a model of a fast ship. The ship model is fitted with a GPS device, a control system, a motor, and a communication system. The case study of the interceptor mounted on two distinct sides at the ship's stern is conducted with various combinations of interceptor blade height (d) between the two sides, including 100% d, 50% d, and 0% d. The test findings consist of model trajectory, velocity, and an IMO standard maneuver. The combination of 100% d at portside, 0% d at starboard side, and the rudder pointing portside at 35 degrees angle resulted in the best tactical diameter, which is 21.49% smaller than without the interceptor.

Keywords: interceptor, maneuverability, open pool free-running test

1 INTRODUCTION

A fast ship, which has a speed greater than the Froude number of 0.4, reduces travel time but has poor maneuverability. According to the findings of the Indonesian National Transportation Safety Committee, the Harapan Baru Express VII fast ship is involved in a collision accident [1]. The report also mentions evidence that indicates the ship started to lose control when it is moving at top speed; therefore, the captain fails to react swiftly, causing it to crash into the trees along the river's edge. It serves as a reminder that the ship's maneuverability is important because fast ships need to be able to change course quickly. A key component in evaluating maneuverability is the turning maneuver [2]. The turning maneuver test shows that high ability is required to quickly change the heading of a fast ship. A negative impact is evident by the fast ship's tendency to have bad turning performances. Based on the above findings, the captain has a limited amount of time to act. The captain would have more time to act if the turning parameters were smaller. The effectiveness of collision avoidance depends on the timing with which a ship initiates maneuvers [3].

The hydrodynamic lift force that supports a fast ship at high speeds generates a shift in motions, which may then lead to an unstable ship attitude and performance [4]. Its excessive motions have been successfully controlled by interceptors. A flat plate with an upward and downward movement is called an interceptor, and it is fastened to the transom [5]. Interceptors modify the fluid flow close to the stern and produce additional normal pressure at the hull's bottom [5]. If one side's interceptor blade is higher than the other, that side's blade also has a higher pressure, which has an impact on maneuvering.

The effect of interceptors on maneuverability has received less attention than the studies of stability and resistance, which have been the subject of numerous experimental and numerical investigations, such as the experimental using a towing tank [5], the design of interceptors for optimum trim control and minimum resistance [6], a study on the influence of interceptors combined with stern flaps [7], a prediction on the hydrodynamic effects of a combination of interceptor and flap on a planing hull using CFD simulation [8], comparing the pressure distribution of a planing hull with and without interceptors using an experimental study [9], and analysis of interceptor impact on prismatic planning hull [10]. In general, the side force produced by the rudder has the main impact on the ship's maneuverability. Not only the rudder affects maneuverability but also the ship's motion [11]. The bow trim ship has a smaller tactical diameter than the stern trim ship.

To examine the interceptor effect on a ship's maneuverability, this study conducts an experimental test in which a scale model is used to measure maneuverability. Since the test is conducted in an open pool, the method is referred to as the open pool free-running model test method. To ensure that the model results reflect the actual situation, the ship model is fitted with a main electric system, a device control system, a signal measurement system, and a communication system. There are many methods to collect the trajectory, such as color object tracking [11] and the image processing method [12]. But both are not appropriate for open pool testing because there is interference from the sunlight, so this study uses a GPS (Global Positioning System) device. A GPS device is used to record the trajectory of the ship, and the trilateration method—which makes use of many satellites—is utilized to find precise locations on the earth’s surface. A GPS device is a useful tool for recording the trajectory of an outside activity [13].

This study examines the impact of interceptor blade-generated stern pressure on a fast ship's maneuverability. The amount of pressure and normal lift produced by the Interceptors blades depends on their heights [6]. The rudders are executed at 35 degrees portside. If the portside's interceptor blades are higher than the starboard side's, the portside will have more lift, and the ship will perform lower turning parameters when turning than the other side. The reference design for the full height (d) of the interceptor blade is 60% of the plate's boundary layer thickness [6]. For the turning maneuver test, either portside or starboard side of the ship, the tests are conducted at full height (100% d), half height (50% d), and without an interceptor (0% d). The IMO's (International Maritime Organization) suggestion is followed while comparing the turning parameters [14]. The open pool free-running test method is used to conduct the model test. The trilateration method with a GPS device is used to collect the trajectory. This study investigates the interceptor phenomenon using a corvette sigma type. The ship has been investigated in numerous studies, such as estimating the motion using a mathematical model [15], the wave load analysis for the ship [16], and numerical analysis of ship motion and strength due to slamming load [17]. The model is fitted with interceptor and rudder instruments. They are calibrated, and the steps are shown in this study.

2 EXPERIMENTAL SETUP

This section delineates the experimental tools and procedures to execute experimentation. The experimental method used in this study follows the recommendation from the ITTC (International Towing Tank Conference) [18]. That method is an open free-running model test, and it uses a GPS tracking method to record the ship's location

2.1 Experimental equipment

The corvette ship type, one of the guard ships in Indonesia, is the model ship used in this study. In this experiment, a scale model ship built at a scale of 1:71.13 is used. The main dimensions between the model scale and the full scale are described in Table 1. The side view of this fiber material model is illustrated in Fig. 1, which is the sheer plan. This twin screw ship has two rudders that help control the ship's course, which is illustrated in Fig. 2. The submerged rudder area is 776 mm^2, and the rudder cross-section is based on the NACA 0021 and 0016 designs. A 48 mm-diameter twin propeller with three blades provides the model's thrust. The model ship has a propulsion system, steering system, control system, interceptor equipment, mini-PC, and GPS equipment that allow an operator to control the ship's course. The location of the ship's center of gravity is taken into account when placing any equipment on the hull, and the model hull space is adjusted. In Fig. 3, the side view, it is possible to observe where the model's equipment is located.

Table 1. Main dimensions

Dimension	Notation	Model scale	Full scale
Length overall	L_{OA}	1.500 m	106.70 m
Length of waterline	L_{WL}	1.407 m	100.10 m
Breadth	B	0.197 m	14.00 m
Draught	T	0.052 m	3.70 m
Service speed	V	1.830 m/s	15.43 m/s

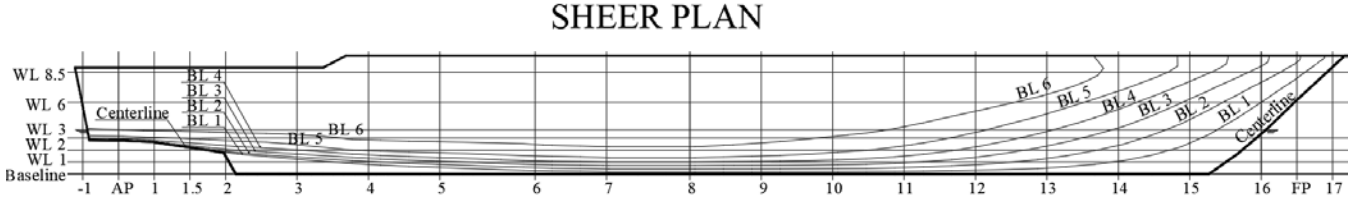

Fig. 1. Sheer plan

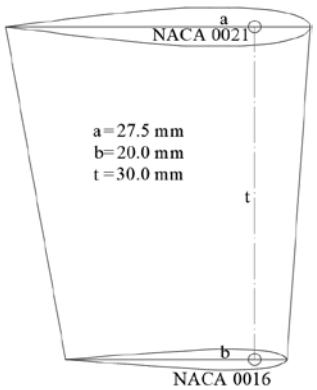

Fig. 2. Model-scale rudder sketch

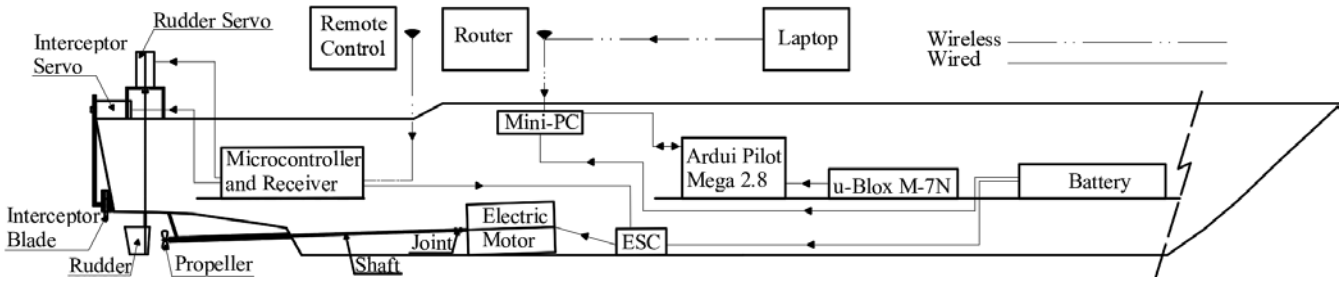

Fig. 3. Side view of the model-scale sketch

An open pond at Institut Teknologi Sepuluh Nopember (ITS) is used for the turning circle test of the model ship. During the test, the water's surface is calm, there is very little wind, and the temperature is not very warm. There is no blockage effect from the pool wall because the test pool area is sufficiently large for the model maneuvering test. The test pool is 35.53 meters wide, 39.73 meters long, 5 meters pool depth, and 4 meters water depth (H), as shown in Fig. 4. To prevent the shallow water effect, the ratio of the water depth (H) to the ship's draught (T) is greater than 4, or H/T > 4.

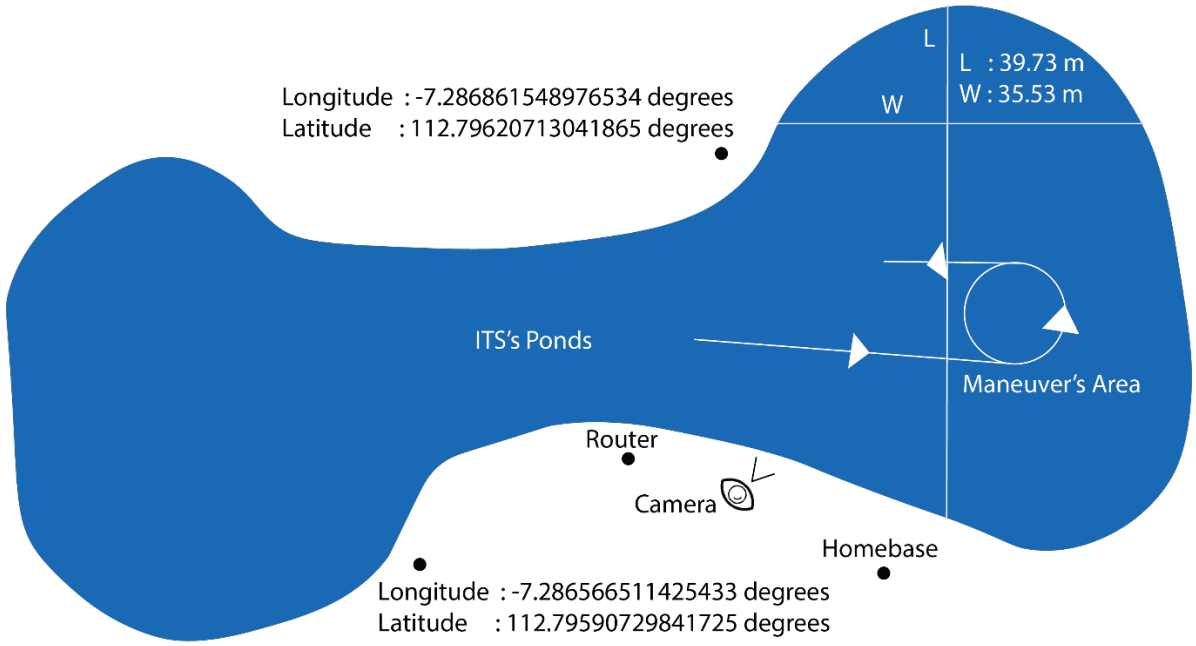

Fig. 4. Top view of the pond sketch

The testing equipment consists of onboard and offboard equipments. Onboard equipment is the entire equipment on board the model ship, while offboard equipment is the equipment on the ground. Offboard equipment consists of a laptop/PC, anemometer, joystick, camera, and router. While the locations of offboard equipment are illustrated in Fig. 4, which also provides the coordinates of the pool location, Homebase is where the laptop and anemometer are located. Using a GPS device and the trilateration method, the location of the ship is determined based on the earth's coordinates that the ship passes through. The interceptor design follows the reference design [6]. The boundary layer thickness (h) is used to determine the full height of the interceptor blade (d), and the boundary layer thickness formula is based on flat plate research [19], as shown in Equation 1.

$$h = 0.382 \frac{L_{WL}}{Re_{L_{WL}}^{0.2}} \quad (1)$$

ReLWL is the Reynolds number, and LWL is the length of the waterline. According to the recommendation, which states that the full height of the interceptor blade (d) ranges from 10% to 60% of the boundary layer's thickness (h) [6], 60% is selected. After that, the interceptor span (S) is calculated using Equation 2.

$$S = d\left(4.0727 + \left(\frac{86.617}{1+\left(\frac{\left(\frac{d}{h}\right)}{0.13}\right)^{2.2648}}\right)\right) \quad (2)$$

According to Equation 1 and 2, the interceptor's full height (d) and span (S) are 17.43 mm and 58.43 mm, respectively. The thickness of interceptor blade is 3 mm. The applied areas of the full and half interceptor blades are 1018.43 mm^2

and 509.22 mm^2, respectively. To see how the interceptor looks, Fig. 5 shows the model-scale interceptor sketch and the applied full height of the interceptor blade.

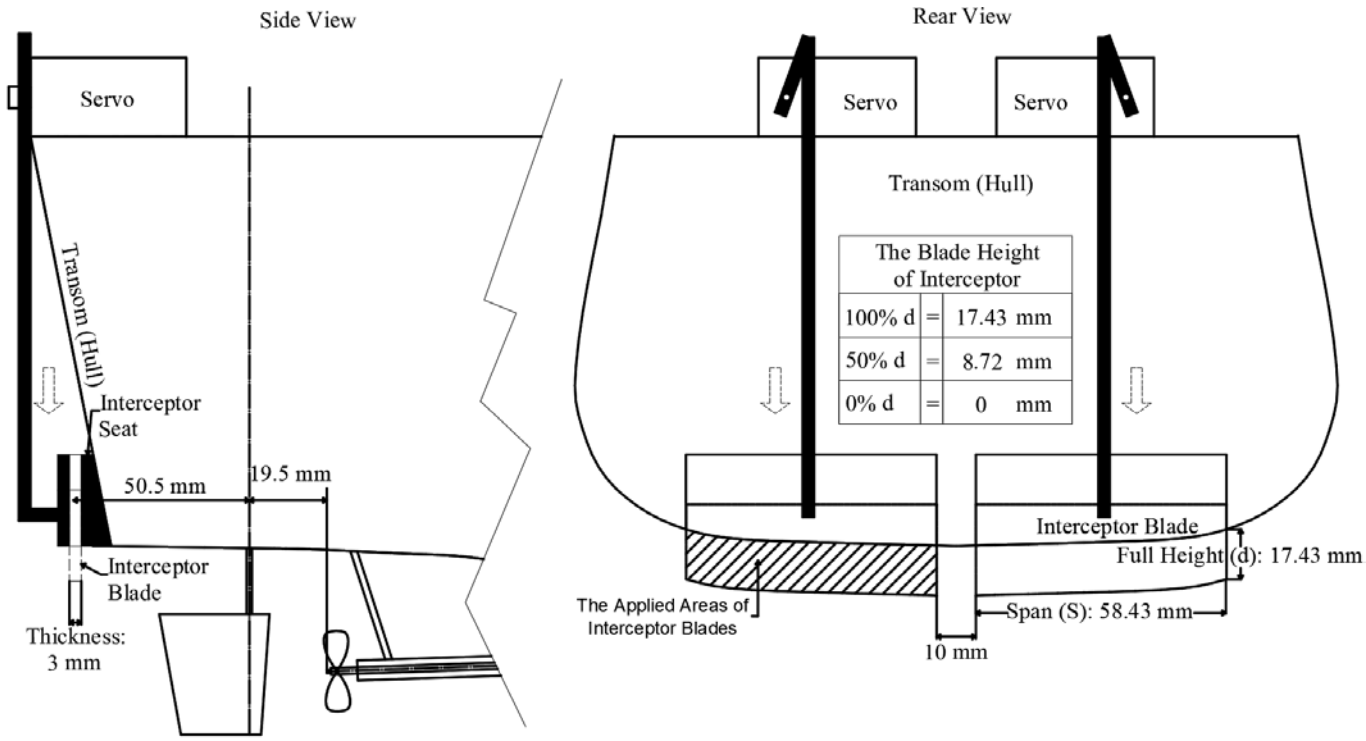

Fig. 5. Interceptor sketch

The model ship is powered by twin screw ship propulsion, so there are two electric motors powering the model ship. The electric motor utilized is “Aquastar 3974-2200 KV DC brushless motor”. Each electric motor has its own Electronic Speed Control (ESC), which is used to control RPM. The ESC utilized is “Seaking V3 RTR 90A”. Both motors operate at 419 RPM, whether in manual or automatic modes. A battery provides power to the ESC. A total of 3 units of Lippo batteries with a 4200 mAh capacity are used, 2 units for the ESC and 1 unit for the mini-PC. The battery is "red Lippo 3S 4200 mAh". There are four servo units to control two rudders and two interceptor blades. The servo is “Metal Gear Toward Pro MG 996R”.

In this investigation, the ship's trajectory is tracked using a GPS device. The “u-Blox M-7N” GPS module, which is driven by an “ArduPilot Mega (APM) 2.8”, is used to record the ship's location and direction. A mini-PC on board controls them, while a laptop on the ground controls the mini-PC via a remote software. A mini-PC is used to save the output data, which is a “Bee-link T4 Pro” mini-PC. The laptop and mini-PC are connected via the router-provided local network.

Using a 2.4G signal and a joystick connected to an on-board receiver, the model ship is operated. Fry Sky Taranis Q X7 and Fry Sky X8R, respectively, are the joystick and receiver that are being used. The rudder servo toggle, automatic switch toggle, microcontroller switch toggle, and main electric motor toggle are the four functioning toggles on the joystick. A Rudder motor toggle operates both rudder servo motors directly. Automatic switch toggle is a toggle to switch manual mode to automatic mode, and vice versa. A microcontroller switch toggle is used to manage which of the interceptor set variations to test. In the experiment, a microcontroller is used as hardware to save and transmit joystick command information. While the receiver is connected to the microcontroller through a board panel. There are two operating modes for microcontrollers: manual and automatic. In manual mode, the joystick is used to directly control the instruments (electric motor and rudder servo). Whereas the instrumentation (electric motor, servo for the rudder, and servo for the interceptor) is controlled in automatic mode by command data inputted into the microcontroller. The voltage value for the electric motor, rudder servo, and interceptor servo is the command information, therefore, it is commonly called the endpoint adjustment. The interceptor variation set is controlled by a joystick, and indicator lamps are functioned to show the selected cases to run. The endpoint adjustment that has been established allows the main electric motor toggle to manually control the electric motor's RPM.

Some software is used in this experiment. (i) "Record Sheets," a program for logging wind velocity, temperature, and time stamp. (ii) "Trajectory Record," a program that records and transforms location data into a time domain. (iii) "Log Data Extraction" software. (iv) ".kml" to ".csv" converter software (v) “Matlab” software. (vi) Remote Access and Remote Control of Computer (RARCC) software, a software that enables laptop control of a mini-PC.

2.2 Experimental procedures

Experimental procedures consist of study cases, tools calibration, testing procedures, and data processing. Both the servos for the interceptor and the rudder need to be calibrated. The calibration steps are shown in this paper.

2.2.1 Study cases

The model ship is propelled by an electric motor that operates at 419 RPM. The distance to the maneuver's area is taken into account, the ship's velocity before executing the rudder is around 2 m/s, and the high speed is a suitable parameter for interceptor testing. The impact of the interceptor blade height on fast ship maneuverability is examined in this study. The turning maneuver with a 35-degree portside rudder serves as the test parameter. Both on the port and starboard sides, the evaluated interceptor blade heights are full height (100% d), half height (50% d), and without interceptor (0% d). The turning parameters to review are tactical diameter, transfer, and advance. The effect of identical interceptor blade heights on both sides is demonstrated by reviewing the turning parameters, which on both sides are 0% d, 50% d, and 100% d. This study is also demonstrated the impact of the different interceptor blade heights on both sides; they are 100% d at portside with 50% d at starboard side and 100% d at portside with 0% d at starboard side. Therefore, Table 2 shows the five different cases that are tested in this study.

Table 2. Case of interceptor height

Case	Interceptor blade height	
	Portside	Starboard side
1	0% d	0% d
2	50% d	50% d
3	100% d	100% d
4	100% d	50% d
5	100% d	0% d

2.2.2 Rudder's servo calibration

The voltage that is inputted into the rudder's servo is set by the calibration of the rudder. This study involves a 35-degree portside turning circle maneuver test, so the servo voltage value of the rudder is set to operate the rudder at 35 degrees portside. A stationary arc and foam blades are the tools for this calibration procedure. The foam blades, which are two pieces of foam linked together at the ends with a bolt to act as a hinge, are the comparison tool for the rudder angle. The following are the procedures for calibrating the rudder's servo: (i) The stationary arc at a 35-degree angle is compared to the foam blades. (ii) One of the foam blades and the rudder seat line up. (iii) The rudder is rotated toward the other foam blades using the joystick. (iv) The voltage is entered into the microcontroller for automatic mode once it is recorded on the joystick's screen. The result, the 35-degree portside rudder requires a 39% endpoint adjustment to be executed.

2.2.3 Interceptor's servo calibration

The purpose of the interceptor's servo calibration is to confirm the variations in the interceptor blade height that want to be tested are correct, both on the port and starboard sides. The following are the procedures for calibrating an interceptor's servos: (i) The joystick, vernier caliper, battery, and ESC are prepared. (ii) After connecting the ESC to the battery, the joystick is turned on. The connection between the servo and the joystick is validated as secure. (iii) The vernier caliper is calibrated to the proper value for the interceptor blade height being compared. (iv) The vernier caliper's blade is applied to the interceptor seat's lip, which is illustrated in Fig. 6. (v) The interceptor blade is released using the joystick. On the joystick's screen, the endpoint adjustment percentage is displayed at the moment the interceptor blade lets off. (vi) The percentage value when the interceptor blade touched the body of the vernier caliper is written down for automatic mode (see Fig. 7). (vii) For each variation of the interceptor blade, steps 1 through 5 are performed for the port and starboard sides. The results are described in Table 3.

Fig. 6. Preparing the vernier caliper

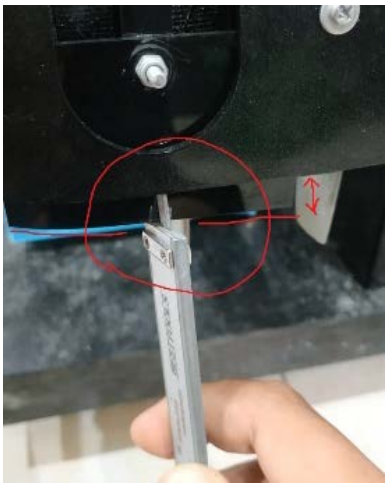

Fig. 7. Interceptor blade is reached vernier caliper's body

Table 3. Interceptor's servo calibration results

The height of interceptor blade (mm)	Percentage of endpoint adjustment (%)	
	Portside	Starboard side
0	-2.5	-27.7
8.72	-66.3	46.2
17.43	-100	86

2.2.4 Testing procedures

The experiment includes three replications. The steps of the testing procedures are as follows: (i) The experimental equipment is prepared, and the pool is in good condition. (ii) The GPS and mini-PC are turned on, and both are solidly connected. (iii) The model is placed on the water's surface and directed to the maneuver's area. (iv) After the router is switched on, the laptop is connected to the mini-PC solidly using the local network. (v) The RARCC software and "Trajectory Record" application are turned on. (vi) The field data are directly recorded using the "Record Sheet" program in the "start trial" command. (vii) The model runs into the maneuver's area, and that procedure utilizes the joystick to manually operate the model. (viii) The model's mode is changed from manual to automatic at the maneuver's area. While the field data are recorded. (ix) The ship made a 3.5-round circle as it rotated. (x) Once the allotted number of rounds is completed, the model's mode is switched from automatic to manual, and it is then run manually to leave the maneuver's area. (xi) The "Trajectory Record" program is terminated. While the field data are recorded. The procedures are depicted schematically in Fig. 8.

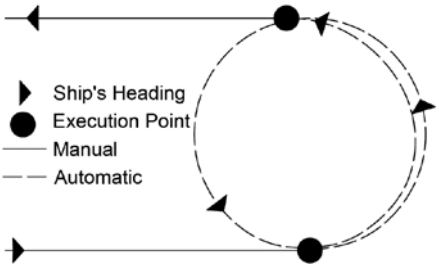

Fig. 8. Schematic of testing procedures

2.2.5 Data processing

The steps involved in processing the data are extracting-rotating, constructing spline models, and specifying-measuring. The extracting-rotating steps are as follows: (i) The "Trajectory Record" software output data is the ".tlog" file type. The information contains degree-based coordinate points (longitude and latitude). (ii) Using the software "Trajectory Record", the output data is saved as a ".kmz" file type from a ".tlog" file type. (iii) Using the "Log Data Extraction" software, the ".kmz" file type is opened. (iv) The coordinates of the maneuver are sorted using the "Record Sheets" program's time record, and then the data is saved as a ".kml" file type. (v) The ".kml" file type is converted to ".csv" using the converter software before opening the coordinates data. (vi) Each degree-based coordinate is converted to meter units by multiplying by 111.319 kilometers, as one degree of the earth's surface corresponds to about 111.319 kilometers [20]. (vii) The trajectory's center is mapped to the origin. (viii) The ship direction of the heading of 0° is pointed in the same direction for every trajectory when switching from manual to automated mode for the first time, so the trajectory rotation is required. Equations 3 and 4 are used to rotate the trajectory, and the rotation procedure is illustrated in Fig. 9.

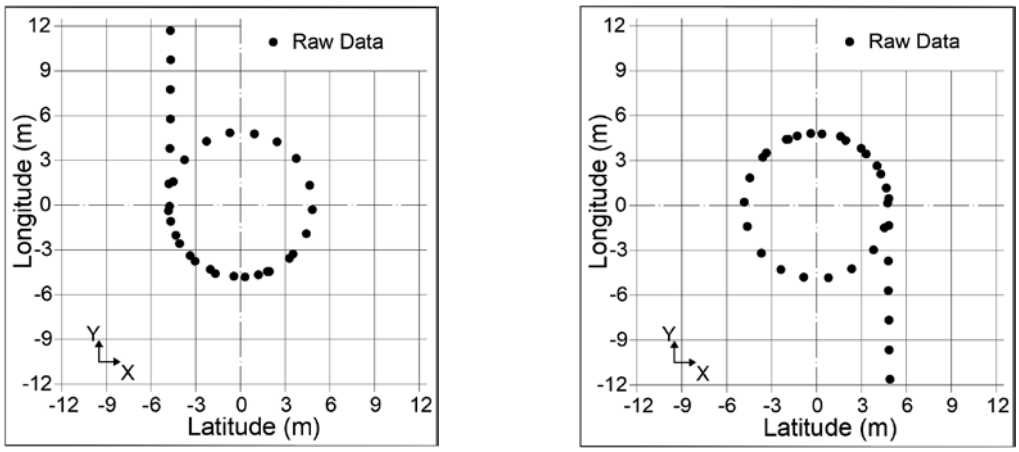

(a) (b)

Fig. 9. Rotating the trajectory: (a) before rotating and (b) after rotating

$$x' = x\cos(\beta) - y\sin(\beta) \quad (3)$$

$$y' = x\sin(\beta) + y\cos(\beta) \quad (4)$$

x and y are the original coordinates, x' and y' are the rotated coordinates, and β is the rotation angular value (degrees). Each point is connected to a line in order to describe the line trajectory; hence, a spline model is created. The steps for constructing a spline model are as follows: (i) The trajectory data are separated into their X and Y coordinates into the time domain, see Fig. 10. (ii) Using "Matlab" software, a spline is created based on the raw data points. The error (the difference between the spline model and raw data) needs to be taken into account because the spline model points are not exactly at the raw data points. (iii) The elevation error is calculated in the same-timestamp X and Y coordinates, and then the standard deviation (σ) is determined, as shown in Equation 5. (iv) A circular trajectory for the ship is generated using the X and Y coordinates from the spline model (see Fig. 11).

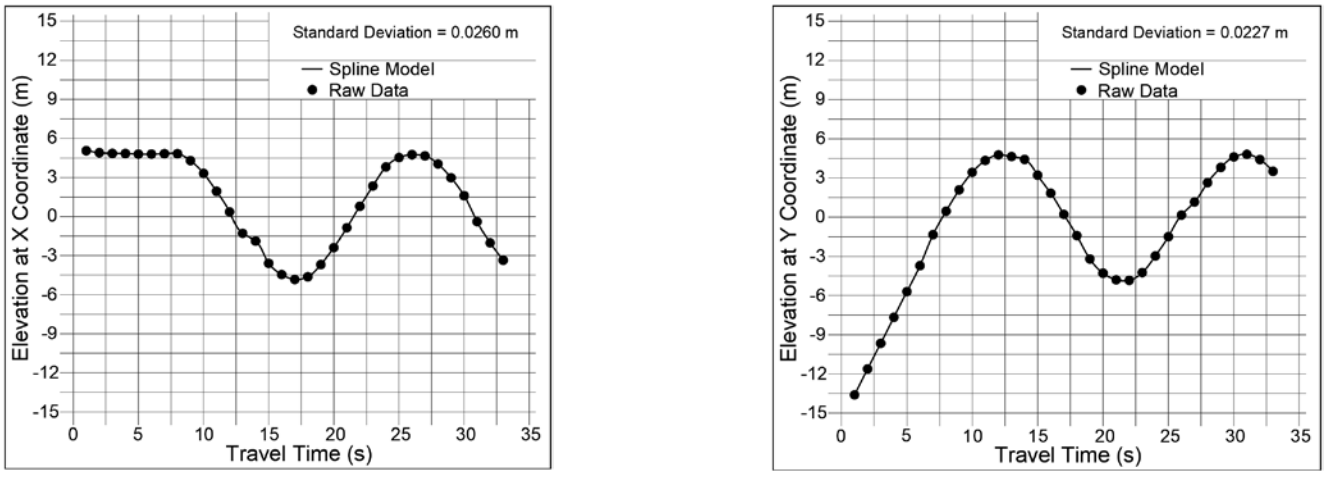

(a) (b)

Fig. 10. The separated data and the standard deviation each coordinate: (a) X coordinate and (b) Y coordinate

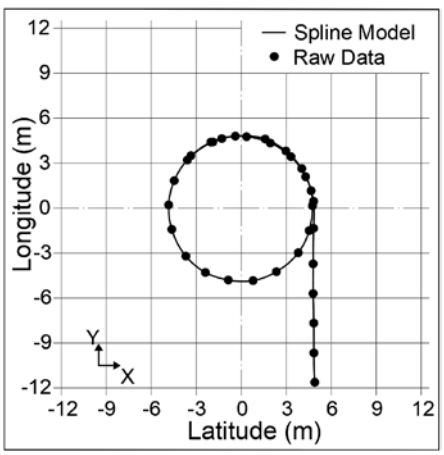

Fig. 11. The spline model and raw data

$$\sigma = \sqrt{\frac{\sum(E_i - \bar{E})^2}{n-1}} \quad (5)$$

Where E_i is error (elevation difference) at the same timestamp, $\bar{E}$ is mean of the error, and n is the data length. The standard deviation is calculated on X and Y coordinates for each variation, see Fig. 10. The specifying-measuring procedures are as follows: (i) The ship's heading coordinates are determined at 0°, 90°, and 180° based on the time record from the "Record Sheets" program. (ii) The turning circle's dimensions are measured, and the parameters are compared. The distance in X coordinates between a direction of 0° and 180° is known as the tactical diameter. Transfer is the distance in X coordinates between the headings of 0° and 90°. Advance is the distance in Y coordinates between the headings of 0° and 90°. Fig. 12 illustrates the results of the procedures for specifying coordinates. (iii) Based on the model spline data, the travel length (L_T) is determined between each point. (iv) The name for each travel length is given; in the following, the length is referred to as steps 1, 2, 3, and so on. See Fig. 13. (v) The ship's translational velocity is calculated after determining the travel times for each step. Equation 6 is used to calculate travel length (L_T), where x_i and y_i are the spline model data points.

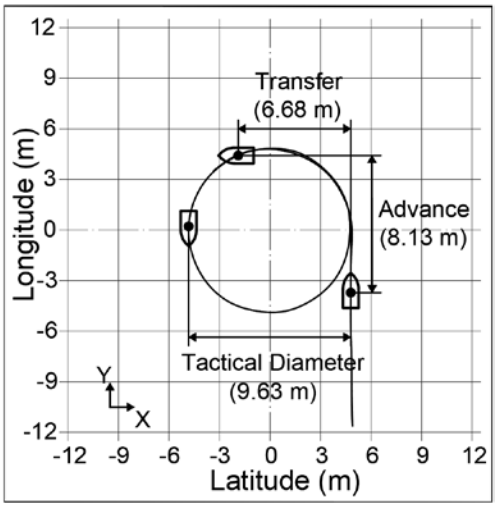

Fig. 12. The specifying and measuring results

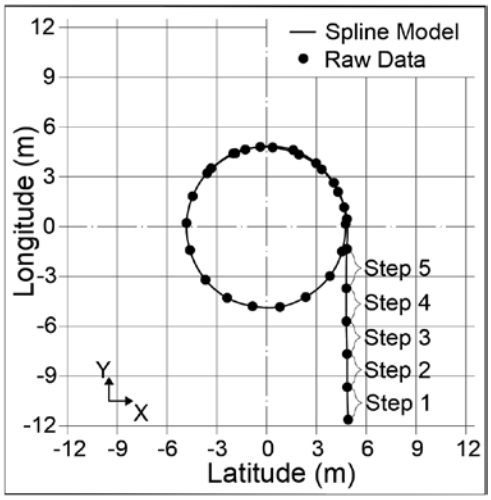

Fig. 13. The line trajectory with the steps

$$L_T = \sqrt{(x_i - x_{i-1})^2 + (y_i - y_{i-1})^2} \quad (6)$$

3 RESULTS AND DISCUSSIONS

At ITS's ponds, a fiber corvette model is tested using the open free-running test method on a 1:71.13 scale model. In order to achieve the best results, the wind and the water's surface are studied in this experiment. The turning maneuver with a 35-degree portside rudder is the test parameter. An investigation of interceptor impact on ship maneuverability is conducted, and the interceptor's dimensions are 58.43 mm in span (S) and 17.43 mm in full height (d). Based on the disparity in interceptor height at the port and starboard sides, Table 2 lists five cases that are investigated. This experiment uses a GPS device to gather the trajectory data. The GPS device effectively captures the maneuver's trajectory, which has a circular shape (see Fig. 14). However, a spline model is developed to represent the line trajectory after data processing. The spline model presents well the line trajectory results, with

standard deviations (the difference between the spline model and the raw data at the same time) are less than 5 cm based on X and Y coordinates in the time domain, which is the standard deviation range of 2.04 mm to 4.90 mm. The standard deviation results are listed in Table 4.

Table 4. Standard deviation of developed spline model

Case	X coordinate (m)			Y Coordinate (m)		
	Rep. 1	Rep. 2	Rep. 3	Rep. 1	Rep. 2	Rep. 3
1	0.0333	0.0260	0.0241	0.0331	0.0429	0.0297
2	0.0238	0.0278	0.0260	0.0312	0.0263	0.0227
3	0.0204	0.0490	0.0239	0.0364	0.0399	0.0313
4	0.0338	0.0322	0.0356	0.0387	0.0356	0.0267
5	0.0315	0.0357	0.0277	0.0219	0.0312	0.0250

The spline model results, which are based on the raw data, effectively depict the interceptor's impact on turning maneuver performance. The tactical diameter, transfer, and advance are measured and shown in Table 5. To observe the trajectory dimension of all cases, Fig. 14 depicts all the line trajectories.

Table 5. Turning parameter results

Case	Tactical diameter (m)			Transfer (m)			Advance (m)		
	Rep. 1	Rep. 2	Rep. 3	Rep. 1	Rep. 2	Rep. 3	Rep. 1	Rep. 2	Rep. 3
1	10.27	9.75	9.91	6.29	5.99	6.78	7.29	5.54	6.52
2	9.8	9.57	9.63	5.77	7.56	6.68	7.64	6.25	8.13
3	8.85	8.79	8.91	4.8	5.41	5.56	6.32	9.16	4.71
4	8.66	8.84	8.4	4.65	3.65	4.14	7.79	6.4	8.36
5	7.78	7.83	7.78	4.71	5.1	4.67	5.58	5.06	7.25

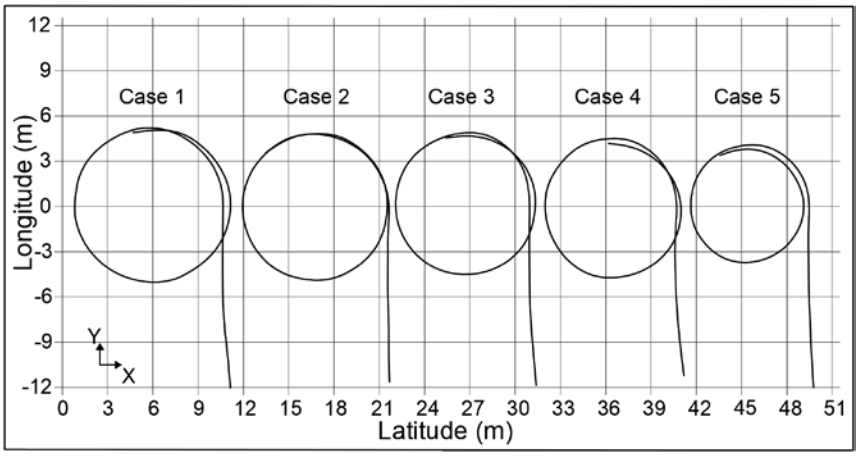

Fig. 14. The line trajectory of all cases

The effects of the blade height variation of the interceptor on turning performances are the main topics of this study. The turning parameters are impacted by the pressure that the interceptor creates in the stern. Case 5 exhibits the lowest turning performance according to the turning parameter results; the turning parameters are reduced in comparison to without an interceptor, namely 21.49% tactical diameter, 30.53% transfer, and 14.42% advance.

In the comparison of identical heights of interceptor blades, Cases 1 through 3, their tactical diameters are 9.91 m, 9.57 m, and 8.79 m, respectively. In Cases 2 and 3, the tactical diameters are reduced by 3.43% and 11.30%, respectively, in comparison to Case 1 (without an interceptor). This advantage is attributed to the interceptor's ability to allow the ship in motion to maintain an even keel or even a condition of trim at the bow [11]. The ship tends to have trim by the stern when traveling at high speeds because the hydrodynamic lift is concentrated in the bow. So that the center of buoyancy is more likely to lie behind the midship, where it is closer to the ship's rudder. However, the interceptor creates pressure in the stern, which adds a normal lift there, so that the ship is inclined to avoid the trim by stern condition. In trim by bow, the ship generates more of the moment's arm to maneuver because the center of buoyancy is farther from the rudder than in trim by stern, where the rudder is the primary mechanism for producing side force for maneuvering.

In the study of the model ship maneuvers to portside, if the height of the interceptor blade is higher on the portside than the starboard side, then the tactical diameter is smaller than without the interceptor. In Cases 4 and 5, the turning parameters are reduced when compared to Case 1. Their tactical diameters are 8.66 meters and 7.78 meters, respectively. Their tactical diameters are decreased by 12.61% and 21.49%, respectively. The interceptor contributes to the turning performance through the pressure it applies. So, it produces more side force when the fluid flows at a lower speed (greater pressure) than the other side. According to Cases 4 and 5, they have a pressure that is greater on the portside than on the starboard side.

Cases 4 and 5 have lower tactical diameters than Case 3, which has the smallest tactical diameter of the cases with identical heights (Cases 1-3). Cases 4 and 5 have 1.48% and 11.49% lower tactical diameters than Case 3. These findings suggest that the interceptor blade needs to be released more toward the portside than the starboard side when the ship wishes to turn there.

The ship's velocity, which is the ship's translational velocity, fluctuates while maneuvering. Figs. 15–19 show the ship's velocity in each case. Executions of the rudder and interceptor are completed in steps of about 3–5. After the execution, the ship's translational velocities fluctuate between 0.66 and 3.02 m/s. While the ship is moving at a velocity of around 2 m/s before the execution. There is a slight but general slowdown in velocity after the execution. In Case 1, the ship is maneuvered at a maximum velocity of 2.02 m/s and a minimum velocity of 0.66 m/s. The maximum and minimum of the ship's maneuvering velocities in Case 2 are 2.58 m/s and 0.65 m/s, respectively. Case 3. the maximum and minimum of the ship's maneuvering velocities are 3.02 m/s and 0.69 m/s, respectively. The maximum and minimum of the ship's maneuvering velocities are 3.02 m/s and 0.71 m/s, respectively in Case 4. 2.53 m/s and 0.66 m/s are the maximum and minimum of the ship's maneuvering velocities in Case 5, respectively.

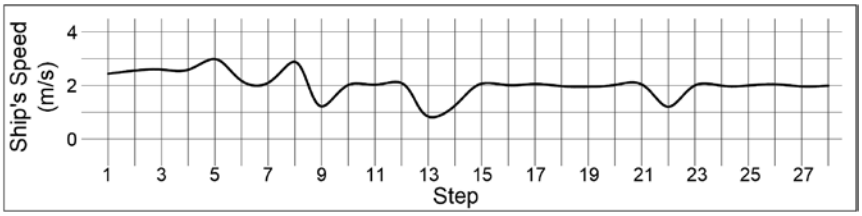

Fig. 15. The ship's velocity of Case 1

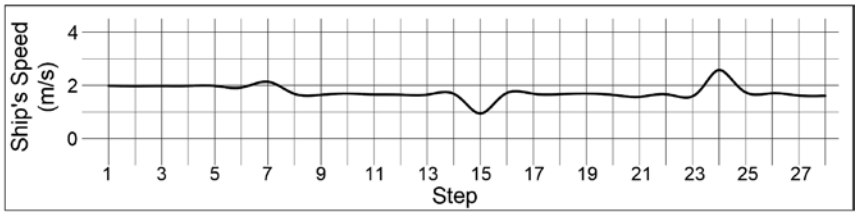

Fig. 16. The ship's velocity of Case 2

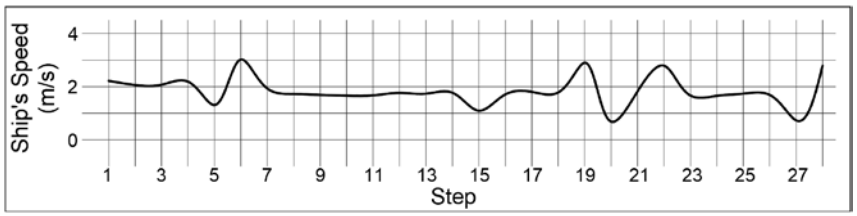

Fig. 17. The ship's velocity of Case 3

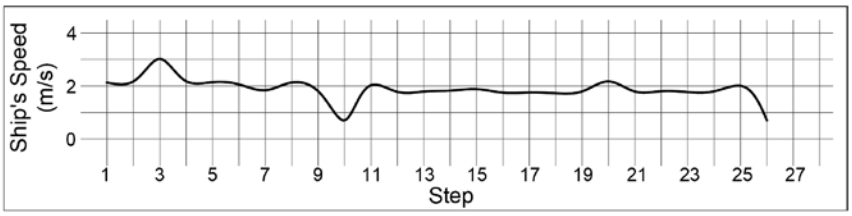

Fig. 18. The ship's velocity of Case 4

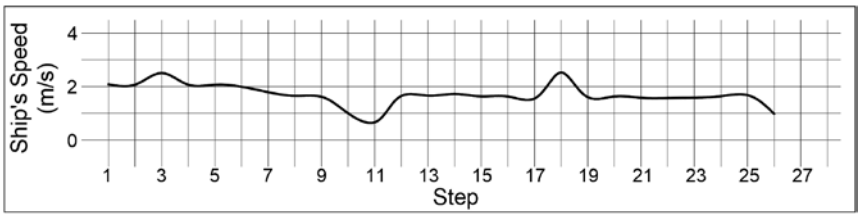

Fig. 19. The ship's velocity of Case 5

After the execution of the rudder and interceptor, the model with interceptor blades has a lower speed than the model without an interceptor. Based on Figs. 15–19, the ship's speed is more stable after Step 12. According to Figs. 15 and 19, Case 1 (without an interceptor) travels at a speed of around 2 m/s, which is higher than Case 5 (the smallest turning parameters), which travels at a speed of about 1.6 m/s. In conclusion, the interceptor slows down the ship's speed during maneuvers because it increases the drag force.

4 CONCLUSIONS

This experiment is an open free-running model test to explore interceptor impacts on maneuvering performance. Five study cases are offered, each case using a different combination of the blade heights of the two interceptors mounted on the port and starboard sides of the stern hull. The turning test reveals that Cases 2 and 3 have a diameter that is approximately 3.43% and 11.30% smaller than Case 1. This phenomenon describes how the trim body created by the interceptor can drastically impact maneuvering performance. In addition, Cases 4 and 5 contribute tactical dimensions that are 1.48% and 11.49% smaller than Case 3. It explains that the different heights of the interceptor blade cause the pressures on the port and starboard sides of the ship to be uneven, which affects the turning maneuver parameters. However, when the interceptor is used, the model's speed slows down because the interceptor increases the body's drag.

5 REFERENCES

[1] Indonesian National Transportation Safety Committee (KNKT Indonesia). (2019). Harapan Baru Express VII collision in the Tanjung Urong River, Tana Tidung, North Kalimantan, Republic of Indonesia. KNKT report no. 18.05.14.03, Jakarta.

[2] Lihua, L., Peng, Z., Songtao, Z., Jia, Y. (2019). Simulation analysis of fin stabilizers on turning circle control during ship turns. Ocean Engineering, vol. 173, 174–182.

[3] Du, L., Banda, O.A.V., Huang, Y., Goerlandt, F., Kujala, P., Zhang, W. (2021). An empirical ship domain based on evasive maneuver and perceived collision risk. Reliability Engineering and System Safety, vol. 213, 107752.

[4] Jacobi, G., Thill, C. H., van't Veer, R., Huijsmans, R. H. M. (2019). Analysis of the influence of an interceptor on the transom flow of a fast ship by pressure reconstruction from stereoscopic scanning PIV. Ocean Engineering, vol. 181, 281–292.

[5] Avci, A. G., Barlas, B. (2019). An experimental investigation of interceptors for a high-speed hull. International Journal of Naval Architecture and Ocean Engineering, vol. 11, no. 1, 256–273.

[6] Mansoori, M., Fernandes, A. C., Ghassemi, H. (2017). Interceptor design for optimum trim control and minimum resistance of planing boats. Applied Ocean Research, vol. 69, 100–115.

[7] Song, K.W., Guo, C., Li, P., Wang, L. (2018). Influence of interceptors, stern flaps, and their combinations on the hydrodynamic performance of a deep-vee ship. Ocean Engineering, vol. 170, 306–320.

[8] Jangam, S. (2022). CFD based prediction on hydrodynamic effects of Interceptor and flap combination on planing hull. Ocean Engineering, vol. 264, 112523.

[9] Seok, W., Park, S. Y., Rhee, S. H. (2020). An experimental study on the stern bottom pressure distribution of a high-speed planing vessel with and without interceptors. International Journal of Naval Architecture and Ocean Engineering, vol. 12, 691–698.

[10] Sahin, O. S., Kahramanoglu, E., Cakici, F. (2022). Numerical evaluation on the effects of interceptor layout and blade heights for a prismatic planing hull. Applied Ocean Research, vol. 127, 103302.

[11] Hafiz, M.A., Sulisetyono, A. (2020). Study of the interceptor's effect on ship manoeuvrability using the open free running test method. Proceedings of 5th International Conference on Marine Technology (SENTA 2020), Surabaya, Indonesia.

[12] Sulisetyono, A. (2018). The Simple Open Free Running Test for the Evaluation of Turning Ship Ability. Proceedings of 6th International Seminar on Ocean and Coastal Engineering, Environmental and Natural Disaster Management (ISOCEEN 2018), Surabaya, Indonesia.

[13] Jin, H., Wu, H., Xu, Z., Huang, W., & Liu, C. (2022). Travel-mode classification based on GPS-trajectory data and geographic information using an XGBoost classifier. IOP Conference Series: Earth and Environmental Science, vol. 1004(1), 012012.

[14] IMO. (2002). Standards for ship manoeuvrability. In Resolution MSC.137(76). International Maritime Organization.

[15] Asfihani, T. et al. (2017). Estimation of the corvette SIGMA motion in missile firing mission. Proceedings of the 5th International Conference on Instrumentation, Control, and Automation (ICA), Yogyakarta, Indonesia, p. 203–207.

[16] Sulisetyono, A., Putranto, T. (2017). Wave Load Analysis of the Corvette Ship in the Sea Water of Indonesia. Applied Mechanics and Materials, vol. 862, 291–295.

[17] Putranto, T., Sulisetyono, A. (2015). Analisa Numerik Gerakan dan Kekuatan Kapal Akibat Beban Slamming Pada Kapal Perang Tipe Corvette (in Indonesian). Kapal, vol. 12, 158–164.

[18] ITTC. (2008). Procedure Free Running Model Tests. In ITTC - Recommended Procedures and Guidelines. International Towing Tank Conference.

[19] Schlichting, H. (1979). Boundary-layer theory (7th ed). McGraw-Hill, New York.

[20] Maria, E., Budiman, E., Haviluddin, Taruk, M. (2020). Measure distance locating nearest public facilities using Haversine and Euclidean Methods. Journal of Physics: Conference Series, vol. 1450, 012080.

Paper submitted: 03.02.2023.

Paper accepted: 19.03.2023.

This is an open access article distributed under the CC BY 4.0 terms and conditions